

# van der Waals interaction of an atom with the internal surface of a hollow submicrometer-size cylinder

Anton Afanasiev and Vladimir Minogin

*Institute of Spectroscopy, Russian Academy of Sciences, 142190 Troitsk, Moscow Region, Russia*

(Received 4 August 2010; published 10 November 2010)

We analyze the van der Waals interaction of an atom with the internal surface of a metal or dielectric submicrometer-sized cylinder and derive closed analytical equations for the van der Waals surface potential and force in the electrostatic approximation. We show that for a concave cylindrical surface the van der Waals potential energy can be up to four times larger than for a flat surface. This result is qualitatively explained by a reduction in the effective distance between the atom and the concave surface compared to that for a flat surface. We also evaluate the shape of an atomic beam propagating inside a hollow dielectric submicrometer-sized cylinder and we propose a scheme that will enable a precise measurement of the van der Waals constant  $C_3$ .

DOI: [10.1103/PhysRevA.82.052903](https://doi.org/10.1103/PhysRevA.82.052903)

PACS number(s): 34.35.+a, 32.70.Jz, 37.90.+j

## I. INTRODUCTION

In recent years there has been increasing interest in the interaction of atoms with submicrometer-sized bodies, such as nanospheres, nanowires, and nanofibers. One of the most important effects that influences the interaction of atoms with the surface of a metallic or dielectric nanobody is the van der Waals interaction [1–18]. This interaction is fundamental in nature and is often viewed as a limit to the Casimir-Polder interaction [5] when the separation between the atom and the surface is less than  $\lambda/2\pi$ , where  $\lambda$  is a wavelength corresponding to a characteristic atomic transition.

In experimental observations of the van der Waals interaction the surface of the macroscopic body is often considered to be a flat surface. Such an assumption is evidently fairly good for atoms located near the surface of the body, i.e., at distances  $x_0$  from the surface that are small when compared to the radius of curvature  $R$  of the surface,  $x_0 \ll R$ . However, for those atoms located at distances comparable to or greater than the surface curvature radius,  $x_0 \gtrsim R$ , the van der Waals interaction potential can differ from that for the flat surface. For a concave surface one should expect an increase in the van der Waals interaction potential. This is explained by a decrease in the effective distance between an atom and the surface. Conversely, one should expect a decrease in the van der Waals interaction potential for a convex surface.

Even though the tendency in the deviation of the van der Waals potential for concave and convex surfaces from that for a flat surface is clear, there is an open question on the quantitative estimate of the contribution of the surface curvature to the energy of the van der Waals interaction. Such a question is of importance for the experiments on the interaction of cold atoms with microtoroids, microspheres and nanospheres, nanowires, and nanofibers [19–25]. In particular, surface curvature can be important in the case of propagation of atoms inside cylindrical surfaces when the interaction time may be long, and accordingly the cumulative effect of the van der Waals interaction can be considerable [26].

Generally, in order to evaluate the van der Waals interaction energy for any type of curved surface one must solve a complicated QED problem in which the retardation effect of the quantized electromagnetic field and the absorbing and dispersing properties of the metal or dielectric medium are

considered [5–7,18]. However, when dealing specifically with nanobodies with sizes less than  $\lambda/2\pi \simeq 100$  nm and assuming that the distance between the atom and the nanobody is of the same order of magnitude, the van der Waals energy can be evaluated using a relatively simple electrostatic approach. To the authors' knowledge, there are no known closed analytical solutions to the van der Waals nonretarded interaction of an atom with a small-sized cylinder. The known general equations for the van der Waals energy for cylindrical surfaces usually reproduce an  $r^{-3}$  dependence for extremely small distances, but they do not give an explicit functional dependence for regions with dimensions similar to the size of the cylinders.

In this paper, we evaluate the effect of surface curvature on the van der Waals interaction potential for an atom in the vicinity of a concave cylindrical surface and we will consider the atom-surface interaction in the electrostatic approximation. Accordingly, we restrict our studies to the case of a hollow micro- or nanocylinder, with radius  $R$  and distances  $x_0$ , between an atom and surface that are small compared to the optical wavelength  $R, x_0 \ll \lambda$ . We assume that the surface of the micro- or nanocylinder is metallic or dielectric. Since we are specifically interested in the role of the surface curvature on the solutions, we neglect the dispersive properties of the medium [27,28].

Derived analytical equations for the van der Waals interaction potential explicitly show that, for a concave cylindrical surface, the reduced effective distance between an atom and the surface increases the magnitude of the van der Waals interaction potential when compared to a flat surface. Quantitatively, we find that, in the central region, the potential of the surface interaction for a concave cylindrical surface can be up to four times higher than for the flat surface. As an example of the use of the derived equations we evaluate the shape of an atomic beam propagating inside a hollow dielectric cylinder and conclude that such a scheme can be used for measuring the van der Waals coefficient  $C_3$ .

## II. ATOMIC DIPOLE NEAR A FLAT SURFACE

As a starting point, we reintroduce the well-known results for the value of the van der Waals interaction energy between an atomic dipole and a flat surface. Consider first a dipole

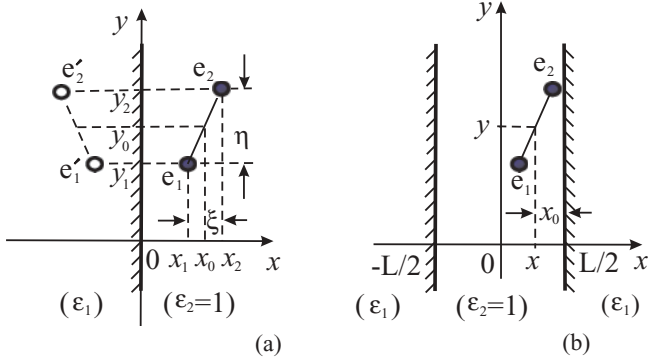


FIG. 1. (a) Position of a dipole and its image near a flat interface separating a conducting medium and vacuum or a dielectric medium with permittivity  $\epsilon_1$  and vacuum. (b) Position of a dipole between two flat metal or dielectric surfaces.

located in the vicinity of the conducting medium as shown in Fig. 1(a). The surface of the conducting medium is assumed to coincide with the  $Oyz$  plane of the reference frame and the atomic dipole lies in the  $Oxy$  plane. The atomic dipole is assumed to be formed by the charges  $e_1 = -e$  and  $e_2 = e$  placed at points  $x_1 = x_0 - \xi/2, y_1 = y_0 - \eta/2$  and  $x_2 = x_0 + \xi/2, y_2 = y_0 + \eta/2$ , respectively.

In a chosen geometry, the electrostatic potential at any point  $P(x, y)$  in the  $Oxy$  plane is defined by the real charges  $e_1$  and  $e_2$  and the image charges  $e'_1 = -e_1 = e$  and  $e'_2 = -e_2 = -e$  located at points  $-x_1, y_1$  and  $-x_2, y_2$ ,

$$\varphi(x, y) = e \left( -\frac{1}{r_1} + \frac{1}{r_2} + \frac{1}{r'_1} - \frac{1}{r'_2} \right), \quad (1)$$

where  $r_i$  and  $r'_i$  are the distances from charges  $e_i$  and  $e'_i = -e_i$  with  $i = 1, 2$  to the observation point  $P(x, y)$ . The potential energy of the dipole after exclusion of the constant interaction energy between the charges  $e_1$  and  $e_2$  is usually defined by [29]

$$U = \frac{1}{2} \sum e_i \varphi'_i = \frac{1}{2} (e_1 \varphi'_1 + e_2 \varphi'_2), \quad (2)$$

where  $\varphi'_1$  and  $\varphi'_2$  are the field potentials produced by the image charges at location points of charges  $e_1$  and  $e_2$ ,

$$\varphi'_1 = e \left( \frac{1}{2x_1} - \frac{1}{\sqrt{(x_1 + x_2)^2 + (y_1 - y_2)^2}} \right), \quad (3)$$

$$\varphi'_2 = e \left( \frac{1}{\sqrt{(x_1 + x_2)^2 + (y_1 - y_2)^2}} - \frac{1}{2x_2} \right). \quad (4)$$

For small distance between the charges  $e_1$  and  $e_2$  constituting an atomic dipole the decomposition of the potential energy (2) up to second order in small distances  $\xi$  and  $\eta$  gives the interaction energy between the dipole, located at position  $x_0, y_0$ , and the conducting plane as

$$U = -\frac{2d_x^2 + d_y^2}{16x_0^3}, \quad (5)$$

where  $d_x = e\xi$  and  $d_y = e\eta$  are the projections of the dipole moment.

Next, by rotating the dipole in the  $Oyz$  plane around the center of the dipole through an arbitrary angle, and taking into account the conservation of the length of the dipole  $d^2 = d_x^2 + d_y^2 + d_z^2$ , one can write out the general equation for the interaction energy in the electrostatic approximation,

$$U = -\frac{2d_x^2 + d_y^2 + d_z^2}{16x_0^3}. \quad (6)$$

Applying this equation to the ground state of the atom and assuming quantum-mechanical averaging over the internal atomic states with

$$\langle d_x^2 \rangle = \langle d_y^2 \rangle = \langle d_z^2 \rangle = \frac{1}{3} \langle d^2 \rangle, \quad (7)$$

one can finally write out the van der Waals potential as

$$U = -\frac{C_3}{x_0^3}, \quad (8)$$

where the quantity

$$C_3 = \frac{\langle d^2 \rangle}{12} \quad (9)$$

is the van der Waals constant for a metal-vacuum interface.

When the flat surface separates the semi-infinite dielectric, with dielectric permittivity  $\epsilon_1$ , and the vacuum semi-infinite region, with  $\epsilon_2 = 1$ , and the atomic dipole is placed in the vacuum region, a similar treatment will reproduce Eq. (8) where the van der Waals constant for the dielectric-vacuum interface is given by

$$C_3 = \frac{(\epsilon_1 - 1) \langle d^2 \rangle}{12(\epsilon_1 + 1)}. \quad (10)$$

It is worth noting that, if one applies a formal transition from the dielectric-vacuum interface to the metal-vacuum interface, one can set  $\epsilon_1 = -\infty$  and, accordingly, obtain a transformation of Eqs. (10) to (9).

Note also, for future comparison, that when an atomic dipole is placed between two flat surfaces as shown in Fig. 1(b) the van der Waals potential can be found by the procedure outlined here as [30]

$$U = -\frac{8C_3}{L^3} \sum_{n=1,3,5,\dots} \left( \frac{1}{(n - 2x/L)^3} + \frac{1}{(n + 2x/L)^3} \right), \quad (11)$$

where  $L$  is the distance between the flat surfaces and  $x = L/2 - x_0$  is the displacement of the dipole with respect to the central plane  $Oy$ . When  $x \rightarrow \pm L/2$  the potential (11) transforms into the potential (8).

### III. ATOMIC DIPOLE INSIDE A CYLINDRICAL SURFACE

Consider now the case where an atomic dipole is placed inside an infinitely long hollow metal cylinder of radius  $R$ . The atomic dipole is at a distance  $\rho_0$  from the center and, accordingly, at a distance  $x_0 = R - \rho_0$  from the surface of the cylinder, as shown in Fig. 2. For this geometry the potential of the electrostatic field produced by a point charge placed inside the cylinder can be found in [31]. For definiteness, we assume that the cylindrical surface is held at zero potential. For

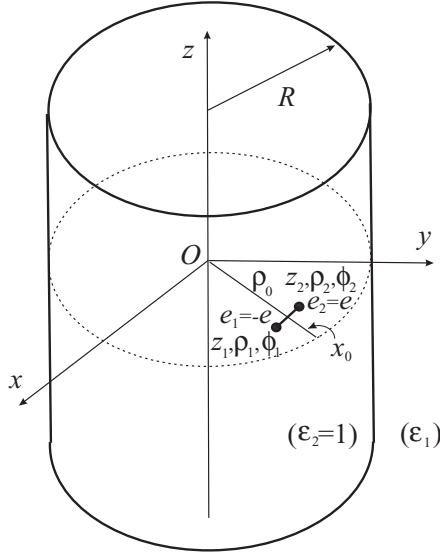


FIG. 2. Position of an atomic dipole inside the cylindrical interface separating the internal vacuum region and the external region with permittivity  $\epsilon_1$ .

our purposes, it is convenient to apply the addition theorem for cylindrical functions and to represent the potential of the charge  $e$ , located at position  $z', \rho', \phi'$ , in a form that explicitly separates the Coulomb part of the potential and the part that is due to the presence of the conducting cylindrical surface. In such a form the potential inside the hollow cylinder at point  $z, \rho, \phi$  is given by

$$\begin{aligned} \varphi(z, \rho, \phi) = & \frac{e}{r} - \frac{2e}{\pi} \int_0^\infty \cos k(z - z') \sum_{m=-\infty}^{+\infty} e^{im(\phi - \phi')} \\ & \times \frac{K_m(kR)}{I_m(kR)} I_m(k\rho) I_m(k\rho') dk. \end{aligned} \quad (12)$$

In this equation,  $r$  is the distance from the charge  $e$  to the observation point and  $K_m(x)$  and  $I_m(x)$  are the modified Bessel functions.

The potential energy of the fluctuating dipole placed inside the conducting cylindrical surface is, again, defined by a general equation (2),

$$U = \frac{1}{2} e(\varphi'_2 - \varphi'_1), \quad (13)$$

where  $\varphi'_1$  is the potential at the position of charge  $e_1 = -e$  and  $\varphi'_2$  is the potential at the position of charge  $e_2 = e$ . The potential at the location point of charge  $e_1$  is defined by Eq. (12) as

$$\begin{aligned} \varphi'_1 = & \frac{2e}{\pi} \int_0^\infty \sum_{m=-\infty}^{+\infty} \frac{K_m(kR)}{I_m(kR)} I_m^2(k\rho_1) dk + \frac{e}{r_{12}} \\ & - \frac{2e}{\pi} \int_0^\infty \cos k(z_1 - z_2) \sum_{m=-\infty}^{+\infty} e^{im(\phi_1 - \phi_2)} \\ & \times \frac{K_m(kR)}{I_m(kR)} I_m(k\rho_1) I_m(k\rho_2) dk. \end{aligned} \quad (14)$$

Here, the first term defines the contribution of charge  $e_1$  and the second and third terms come from the contribution of charge  $e_2 = e$ , with  $r_{12}$  being the distance between the

charges. The potential at the location point of charge  $e_2$  is defined by Eq. (12) as

$$\begin{aligned} \varphi'_2 = & \frac{2e}{\pi} \int_0^\infty \cos k(z_2 - z_1) \sum_{m=-\infty}^{+\infty} e^{im(\phi_2 - \phi_1)} \frac{K_m(kR)}{I_m(kR)} I_m(k\rho_1) \\ & \times I_m(k\rho_2) dk - \frac{e}{r_{12}} - \frac{2e}{\pi} \int_0^\infty \sum_{m=-\infty}^{+\infty} \frac{K_m(kR)}{I_m(kR)} I_m^2(k\rho_2) dk. \end{aligned} \quad (15)$$

The first and second terms define the contribution of charge  $e_1$  and the third term comes from the contribution of charge  $e_2 = e$ , with  $r_{12}$  again being the distance between the charges.

The potential energy of the dipole located inside the concave cylindrical surface after extraction of the constant interaction energy between the charges,  $e_1 = -e$  and  $e_2 = e$ , is therefore given by

$$\begin{aligned} U = & -\frac{e^2}{\pi} \int_0^\infty \sum_{m=-\infty}^{+\infty} \frac{K_m(kR)}{I_m(kR)} [I_m^2(k\rho_1) + I_m^2(k\rho_2) \\ & - 2 \cos k(z_2 - z_1) \cos m(\phi_2 - \phi_1) I_m(k\rho_1) I_m(k\rho_2)] dk. \end{aligned} \quad (16)$$

Taking into account that the size of the atomic dipole is much less than all the other sizes in the considered geometry, we introduce the projections  $\xi, \eta, \zeta$  on axes  $x, y, z$  of the distance between the charges and expand the integrand (16) up to second order in small distances  $\xi, \eta, \zeta$ . This gives the potential energy of the atomic dipole as

$$\begin{aligned} U = & -\frac{1}{\pi} \int_0^\infty \sum_{m=-\infty}^{+\infty} \frac{K_m(kR)}{I_m(kR)} \left\{ \frac{k^2}{4} [I_{m-1}(k\rho_0) + I_{m+1}(k\rho_0)]^2 \right. \\ & \times (d_x \cos \phi_0 - d_y \sin \phi_0)^2 + I_m^2(k\rho_0) \\ & \left. \times \left[ \frac{m^2}{\rho_0^2} (d_x \sin \phi_0 + d_y \cos \phi_0)^2 + k^2 d_z^2 \right] \right\} dk, \end{aligned} \quad (17)$$

where  $d_x = e\xi$ ,  $d_y = e\eta$ , and  $d_z = e\zeta$  are the projections of the dipole moment and  $\rho_0, \phi_0$  are the cylindrical coordinates of the center of the dipole. For the ground state of the atom, the van der Waals potential after averaging over the atomic transitions, taking into account Eq. (7) and following some simplification, can be written as

$$\begin{aligned} U = & -\frac{2C_3}{\pi} \int_0^\infty \sum_{m=-\infty}^{+\infty} \frac{K_m(kR)}{I_m(kR)} \\ & \times [I_{m-1}^2(k\rho_0) + 2I_m^2(k\rho_0) + I_{m+1}^2(k\rho_0)] k^2 dk, \end{aligned} \quad (18)$$

where the van der Waals constant  $C_3$  is defined by Eq. (9). The van der Waals potential, as a function of distance from the cylindrical surface, can be written as

$$U = -\frac{C_3}{x_0^3} \mu, \quad (19)$$

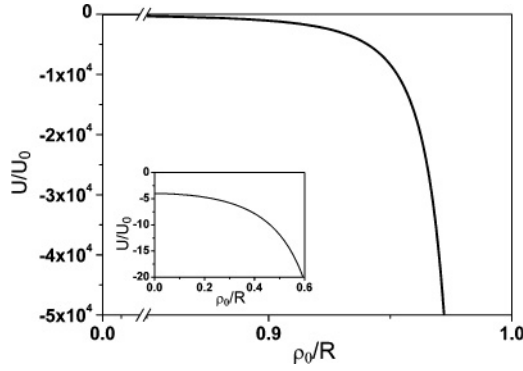


FIG. 3. The van der Waals potential for an atom placed inside a concave cylindrical surface as a function of distance from the center of the cylinder,  $U_0 = C_3/R^3$ .

where the quantity  $\mu$ , which we call the internal cylindrical surface factor, is

$$\mu = \frac{2x_0^3}{\pi} \int_0^\infty \sum_{m=-\infty}^{+\infty} \frac{K_m(kR)}{I_m(kR)} \times [I_{m-1}^2(k\rho_0) + 2I_m^2(k\rho_0) + I_{m+1}^2(k\rho_0)] k^2 dk \quad (20)$$

and  $\rho_0 = R - x_0$ .

If the cylindrical surface separates the internal vacuum region and the outer dielectric medium, which has a permittivity  $\varepsilon_1$ , and the atom is placed in the internal region as shown in Fig. 2, similar calculations will lead to Eqs. (18)–(20), where the van der Waals constant  $C_3$  is defined by Eq. (10).

The van der Waals potential for an atom placed inside a cylindrical surface, as a function of the radial coordinate, is shown in Fig. 3. A quantitative deviation of the cylindrical surface potential from that for a flat surface can be seen from the position dependence of the internal cylindrical surface factor, as shown in Fig. 4. From Fig. 4 it is evident that the potential for a concave cylindrical surface coincides with that for a flat surface at  $\rho_0 \rightarrow R$  when  $\mu \rightarrow 1$  and exceeds that for a flat surface by a factor of 4 near the center of the cylinder.

Figure 5 shows a comparison between the van der Waals potentials determined for two distinct cases (i.e., that of a cylinder of diameter  $2R$  and that of two planes separated by

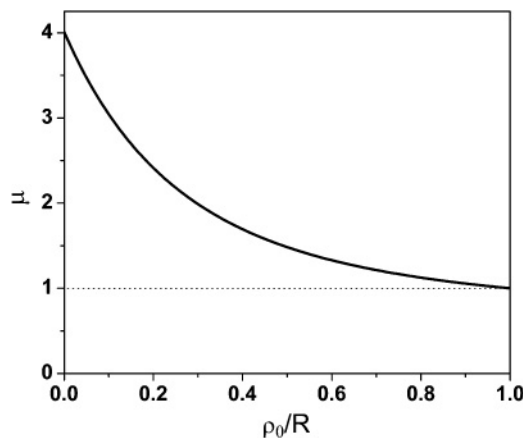


FIG. 4. The internal cylindrical surface factor  $\mu$  as a function of distance from the center of the cylinder.

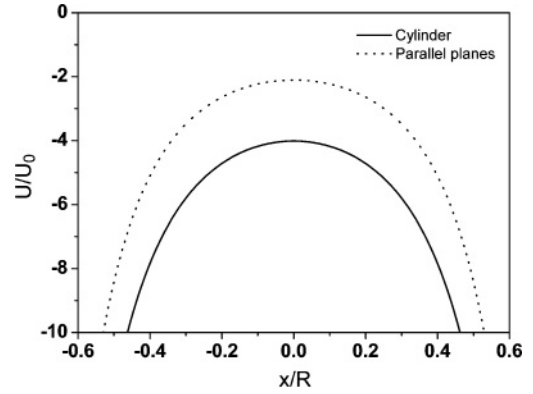


FIG. 5. Dependence of the van der Waals potential on the displacement of an atom from the axis of the cylindrical surface of diameter  $2R$  (solid line) and from the central plane surrounded by two parallel flat surfaces separated by distance  $L = 2R$  (dashed line).

a distance  $L = 2R$ ). In both cases, the qualitative behavior of the potential is similar although the absolute value of the potential for the cylindrical surface exceeds that for the two planes by a factor of 2 near the central region. The twofold increase in the magnitude of the potential as compared to that for the two-plane case corresponds to a value of the cylindrical surface factor equal to 4 in the central region. Qualitatively, the value of the cylindrical surface factor  $\mu$  can be understood by comparing the cylindrical surface surrounding the atom with two planes symmetrically displaced from the atom to the left and right, as shown in Fig. 1(b). In the case of two planes, the surface factor is twice as high compared to that for a single plane [30]. Since the cylindrical surface can be approximately treated as two pairs of planes symmetrically displaced from the atom in directions  $\pm x, \pm y$ , it is natural to expect the appearance of a factor of  $2 \times 2 = 4$  in this case.

We note here that, in previous works dealing with the interaction between an atom or molecule and a cylindrical surface, the electrostatic approximation was typically considered for the case of the atom very close to the external surface of the microcylinder. In this case dependence of the van der Waals potential on the distance between the atom and the surface  $x_0$  was reduced to the known  $x_0^{-3}$  dependence for a flat surface [15,32]. Position dependence of the potential for the concave cylindrical surface over a broad range of distances was considered in [16]. However, in Ref. [16] the van der Waals potential considered at the axis of the cylinder as a function of the cylinder radius  $R$  exhibited  $R^{-2}$  behavior. Such behavior contradicts the  $R^{-3}$  dependence shown in Eq. (19) and the  $L^{-3}$  dependence shown in Eq. (11).

The van der Waals potential for a cylindrical surface as determined here can be used to find the corresponding force,  $F = -\partial U/\partial \rho_0$ , on the atomic dipole:

$$F = \frac{2C_3}{\pi} \int_0^\infty \sum_{m=-\infty}^{+\infty} \frac{K_m(kR)}{I_m(kR)} \{I_{m-1}(k\rho_0)[I_{m-2}(k\rho_0) + 3I_m(k\rho_0)] + I_{m+1}(k\rho_0)[I_{m+2}(k\rho_0) + 3I_m(k\rho_0)]\} k^3 dk. \quad (21)$$

When considered as a function of distance from the cylindrical surface, the force can be written as a product of the force for a

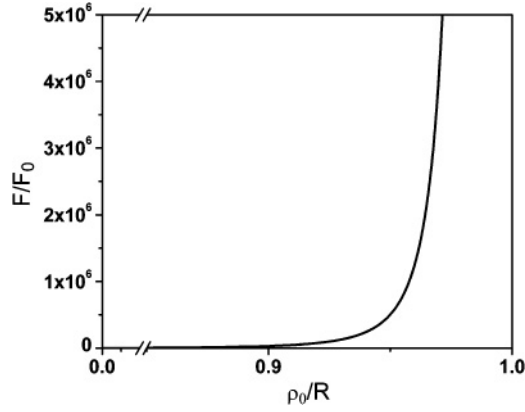


FIG. 6. Dependence of the van der Waals force on the radial coordinate for an atom placed inside a cylindrical surface. The force is normalized to  $F_0 = C_3/R^4$ .

flat surface and the internal cylindrical surface factor  $\nu$ ,

$$F = \frac{3C_3}{x_0^4} \nu, \quad (22)$$

where

$$\nu = \frac{2}{3\pi} x_0^4 \int_0^\infty \sum_{m=-\infty}^{+\infty} \frac{K_m(kR)}{I_m(kR)} \{I_{m-1}(k\rho_0)[I_{m-2}(k\rho_0) + 3I_m(k\rho_0)] + I_{m+1}(k\rho_0)[I_{m+2}(k\rho_0) + 3I_m(k\rho_0)]\} k^3 dk \quad (23)$$

and  $\rho_0 = R - x_0$ .

The position dependence of the force is shown in Fig. 6. Figure 7 shows the position dependence of the cylindrical surface factor  $\nu$ . At  $\rho_0 \rightarrow R$  the force for a cylindrical surface coincides with that for a flat surface and  $\nu \rightarrow 1$ . Near the center of the cylinder the force is zero due to the axial symmetry of the surface. The factor  $\nu$  reaches its maximum value of about 1.2 at  $x_0 \simeq 0.4 R$ ; that is, at this distance the force on the atom

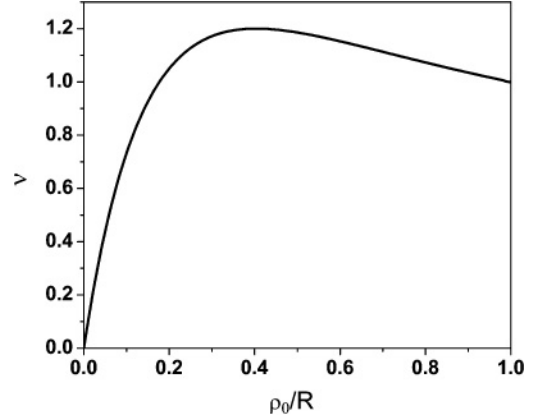


FIG. 7. The cylindrical surface factor  $\nu$  as a function of distance from the center of the cylinder.

is 1.2 times larger for a concave-shaped cylindrical surface than for a flat surface.

#### IV. PROPAGATION OF ATOMS INSIDE A CYLINDRICAL SURFACE

The aforementioned analytical evaluations of the van der Waals potential and force for the interaction between an atom and a submicrometer-sized concave cylindrical surface can be used for comparison with experimental data in measurements of the van der Waals coefficient  $C_3$ . In known measurements of  $C_3$  the van der Waals interaction was mostly assumed to originate from the interaction between an atom and a flat surface. Shih and Parsegian [33] reported on a measurement of  $C_3$  in an experiment on the deflection of a thermal atomic beam by a large-sized gold cylindrical surface which they treated as flat. A measurement of the van der Waals interaction between an atom and a surface has also been done via spectroscopic studies of Rydberg atoms in a micron-sized, parallel-plate metallic cavity [30,34]. Landragin *et al.* [35] measured the

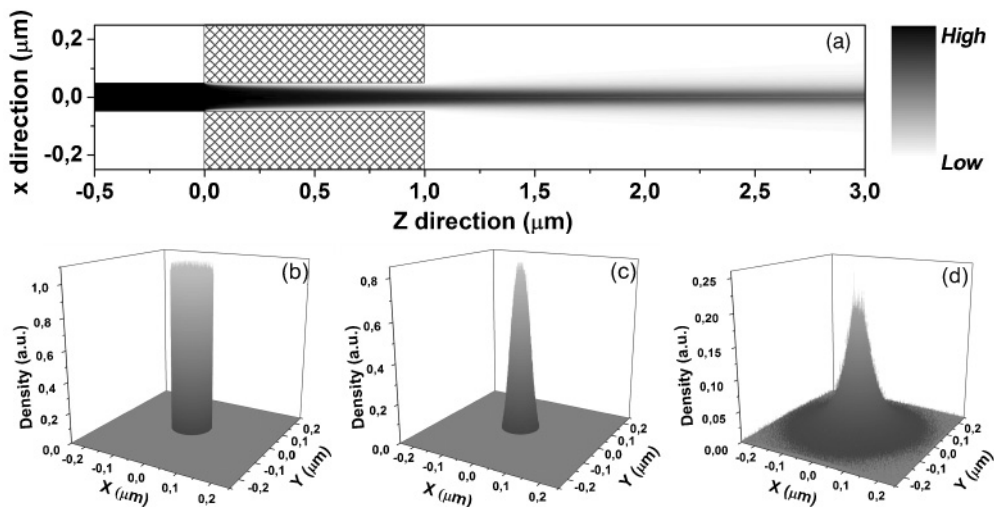


FIG. 8. (a) Profile of an atomic beam propagating through a dielectric cylinder of radius  $R = 50$  nm and length  $l = 1 \mu\text{m}$ ; density of atoms in the cross section of the beam at distance (b)  $z = 0$  nm, (c)  $z = 1 \mu\text{m}$ , and (d)  $z = 6 \mu\text{m}$ .



van der Waals potential for cold atoms released from a magneto-optical trap (MOT) and deflected off a dielectric prism. A very precise measurement technique was developed based on atom reflection by material surfaces [36,37] and scattering of atoms by material gratings [38].

As an example, we will now consider the mechanical action of the concave cylindrical surface potential on an atomic beam propagating inside a small-sized hollow cylinder. In our scheme, shown in Fig. 8, a collimated atomic beam propagates inside a short, hollow, dielectric cylinder. During propagation the atoms gain transverse velocity due to their attraction to the cylindrical surface through the van der Waals force. The bottom plots in Fig. 8 show numerical simulations of the atomic beam density at three different cross sections for a beam of Cs atoms propagating with a longitudinal velocity  $v_z = 50$  m/s through a hollow dielectric cylinder of radius  $R = 50$  nm and length  $l = 1$   $\mu$ m. For evaluation purposes, the van der Waals coefficient is taken to correspond to the interaction between ground-state Cs atoms and fused silica, i.e.,  $C_3 = 1.56$  kHz  $\mu$ m<sup>-3</sup> [39].

Computer simulations for these parameters show that propagation of an atomic beam through the hollow, submicrometer-sized cylinder can result in a considerable increase in the atomic transverse velocities due to the attractive van der Waals force. Accordingly, the transverse distribution of the atomic beam density can be considerably modified with a clear separation over the narrow internal section near the cylinder axis and a relatively broad pedestal as shown in Figs. 8(b)–8(d). Computer simulation also shows that the most profound modification of the atomic beam density occurs in the beam cross sections located at the distances exceeding the length of the cylinder tube as, for example, can be seen in Fig. 8(d). This happens when at sufficiently long propagation time the transverse velocity distribution modified by the van der Waals forces transforms into the modified transverse coordinate distribution. Therefore numerical simulations based on the

derived analytical evaluations prove that a measurement of the atomic beam transverse density profile at different cross sections can be viewed as a sensitive tool to determine the van der Waals coefficient  $C_3$ . In the proposed scheme there can be technical difficulties associated in particular with outgassing of the submicrometer-diameter tubes. However, in the example considered the length of the tube chosen is so small that the achievement of UHV should be a realistic task.

## V. CONCLUSION

The evaluation of the van der Waals interaction using an electrostatic approximation, as presented in this paper, yields a closed analytical representation for the van der Waals potential and force for concave micro- or nanocylinders. The derived potential shows that the energy of the van der Waals interaction between an atom and a concave cylindrical surface can be up to four times higher than that for a flat surface and up to twice as high as that for two parallel flat surfaces.

Computer simulations of atomic beam propagation inside a small-sized, cylindrical channel in bulk material shows that the van der Waals force can produce a sharp transformation of the atomic beam profile, with a clear separation of an internal narrow peak from a broad pedestal. This transformation of the atomic beam transverse density profile is related to the strength of the van der Waals interaction and can accordingly be used for measurements of the coefficient  $C_3$ .

## ACKNOWLEDGMENTS

This work was supported by the Russian Foundation for Basic Research under Grants No. 09-02-13539, No. 09-02-01022, No. 08-02-00871, No. 08-02-00653 and by a grant of the President of Russia (Grant No. MK-1514.2009.2). We are grateful to V. I. Balykin and P. N. Melentiev for helpful discussions.

- 
- [1] J. E. Lennard-Jones, *Trans. Faraday Soc.* **28**, 334 (1932).
  - [2] F. London, *Trans. Faraday Soc.* **33**, 8b (1937).
  - [3] J. Bardeen, *Phys. Rev.* **58**, 727 (1940).
  - [4] H. Margenau and W. G. Pollard, *Phys. Rev.* **60**, 128 (1941).
  - [5] H. B. G. Casimir and D. Polder, *Phys. Rev.* **73**, 360 (1948).
  - [6] I. E. Dzyaloshinskii, E. M. Lifshitz, and L. Pitaevskii, *Adv. Phys.* **10**, 165 (1961).
  - [7] I. E. Dzyaloshinskii, E. M. Lifshitz, and L. P. Pitaevskii, *Sov. Fiz. Usp.* **4**, 153 (1961).
  - [8] J. Mahanty and B. W. Ninham, *Dispersion Forces* (Academic, London, 1976).
  - [9] D. Langbein, *Theory of van der Waals Attraction* (Springer-Verlag, Berlin, 1974).
  - [10] H. Margenau and N. R. Kestner, *Theory of Intermolecular Forces* (Pergamon, Oxford, 1971).
  - [11] G. C. Maitland, M. Rigby, E. B. Smith, and W. Wakeham, *Intermolecular Forces: Their Origin and Determination* (Clarendon, Oxford, 1981).
  - [12] T. Kihara, *Intermolecular Forces* (Wiley, Chichester, 1978).
  - [13] W. A. Steele, *The Interaction of Gases with Solid Surfaces* (Pergamon, Oxford, 1974).
  - [14] J. G. Dash, *Films on Solid Surfaces. The Physics and Chemistry of Physical Adsorption* (Academic, New York, 1975).
  - [15] A. M. Marvin and F. Toigo, *Phys. Rev. A* **25**, 782 (1982).
  - [16] H. Nha and W. Jhe, *Phys. Rev. A* **56**, 2213 (1997).
  - [17] M. Boustimi, J. Baudon, P. Candori, and J. Robert, *Phys. Rev. B* **65**, 155402 (2002).
  - [18] S. Y. Buhmann, H. T. Dung, and D.-G. Welsch, *J. Opt. B* **6**, S127 (2004).
  - [19] K. P. Nayak, P. N. Melentiev, M. Morinaga, F. L. Kien, V. I. Balykin, and K. Hakuta, *Opt. Express* **15**, 5431 (2007).
  - [20] T. Aoki, A. S. Parkins, D. J. Alton, C. A. Regal, B. Dayan, E. Ostby, K. J. Vahala, and H. J. Kimble, *Phys. Rev. Lett.* **102**, 083601 (2009).
  - [21] K. P. Nayak and K. Hakuta, *New J. Phys.* **10**, 053003 (2008).
  - [22] V. G. Minogin and S. Nic Chormaic, *Laser Phys.* **20**, 32 (2010).
  - [23] L. Russell, D. A. Gleeson, V. G. Minogin, and S. Nic Chormaic, *J. Phys. B* **42**, 185006 (2009).
  - [24] M. Morrissey, K. Deasy, Y. Wu, S. Chakrabarti, and S. Nic Chormaic, *Rev. Sci. Instrum.* **80**, 053102 (2009).
  - [25] E. Vetsch, D. Reitz, G. Sagué, R. Schmidt, S. T. Dawkins, and A. Rauschenbeutel, e-print [arXiv:0912.1179v2](https://arxiv.org/abs/0912.1179v2).

- [26] P. N. Melentiev, A. V. Zablotskiy, D. A. Lapshin, E. P. Sheshin, A. S. Baturin, and V. I. Balykin, *Nanotechnology* **20**, 235301 (2009).
- [27] J. M. Wylie and J. E. Sipe, *Phys. Rev. A* **32**, 2030 (1985).
- [28] M. Fichet, F. Schuller, D. Bloch, and M. Ducloy, *Phys. Rev. A* **51**, 1553 (1995).
- [29] J. D. Jackson, *Classical Electrodynamics* (Wiley, New York, 1998).
- [30] C. I. Sukenik, M. G. Boshier, D. Cho, V. Sandoghdar, and E. A. Hinds, *Phys. Rev. Lett.* **70**, 560 (1993).
- [31] J. A. Hernandez and A. K. T. Assis, *J. Electrostat.* **63**, 1115 (2005).
- [32] M. Boustimi, J. Baudon, and J. Robert, *Phys. Rev. B* **67**, 045407 (2003).
- [33] A. Shih and V. A. Parsegian, *Phys. Rev. A* **12**, 835 (1975).
- [34] V. Sandoghdar, C. I. Sukenik, E. A. Hinds, and S. Haroche, *Phys. Rev. Lett.* **68**, 3432 (1992).
- [35] A. Landragin, J.-Y. Courtois, G. Labeyrie, N. Vansteenkiste, C. I. Westbrook, and A. Aspect, *Phys. Rev. Lett.* **77**, 1464 (1996).
- [36] V. Druzhinina and M. DeKieviet, *Phys. Rev. Lett.* **91**, 193202 (2003).
- [37] A. K. Mohapatra and C. S. Unnikrishnan, *Europhys. Lett.* **73**, 839 (2006).
- [38] V. P. A. Lonij, W. F. Holmgren, and A. D. Cronin, *Phys. Rev. A* **80**, 062904 (2009).
- [39] F. L. Kien and K. Hakuta, *Phys. Rev. A* **75**, 013423 (2007).